Available online at www.sciencedirect.com

ScienceDirect

Energy Procedia 77 (2015) 717 – 724

Energy Procedia

5th International Conference on Silicon Photovoltaics, SiliconPV 2015

# Quantification of front side metallization area on silicon wafer solar cells for background plating detection

Martin Heinrich[a,*], Achim Kraft[b], Martin Lieder[b], Bram Hoex[c], Armin G. Aberle[d], Markus Glatthaar[b]

[a]*Now at Department of Microsystems Engineering – IMTEK, University of Freiburg, Georges-Köhler-Allee 106, 79110 Freiburg, Germany*
[b]*Fraunhofer Institute for Solar Energy Systems,Heidenhofstr. 2, 79110 Freiburg, Germany*
[c]*Now at School of Photovoltaic and Renewable Energy Engineering, University of New South Wales, Kensington NSW 2052, Australia*
[d]*Solar Energy Research Institute of Singapore, National University of Singapore, 7 Engineering Drive 1, Block E3A, Singapore 117574, Singapore*

**Abstract**

This work describes a method to measure the metallized area on the front side of silicon wafer solar cells. The method is especially applicable to detect and quantify background plating, which can occur in the production of solar cells with plated front-side metallization. The metallized area of plated solar cells is determined by an image processing algorithm ("MetDetect") using images of the solar cell front side obtained by a simple commercially available flatbed scanner. The algorithm is verified by the comparison of scanned images from test samples with microscope images. Furthermore a correlation of the metallized area with the measured short-circuit current density of the samples justifies the proposed method. With "MetDetect" a precise quantification of the background plating on the plated solar cell front side can be realized. It is suitable for inline inspection in solar cell production or quantification of pinholes and cracks in the surface dielectric. In this work "MetDetect" is applied to corroborate the observation that background plating of solar cells with a nickel copper front side metallization can surprisingly be removed during plating by a thin Sn-capping.


Peer review by the scientific conference committee of SiliconPV 2015 under responsibility of PSE AG

*Keywords:* Front side metallization; Light induced plating; Background plating; Nickel; Copper; Tin; Shading; Metallized area

* Corresponding author. Tel.: +49 761 203 7213; fax: +49 761 203-7222.
*E-mail address:* martin.heinrich@imtek.uni-freiburg.de
The research was performed while M. Heinrich was at [b] and B. Hoex at [d].


Peer review by the scientific conference committee of SiliconPV 2015 under responsibility of PSE AG
doi:10.1016/j.egypro.2015.07.102

## 1. Introduction

Direct plating is currently intensively investigated as an alternative industrial metallization method to screen printing [1]. Extremely small finger widths with high aspect ratios as well as silver free front side metallization of solar cells are possible using plating [2–4].

The plating of the metal occurs only at spots on the wafer surface which are not electrically isolated, e.g. at a metal seed layer or bare Si [5]. A dielectric layer (such as a $SiN_x$ passivation layer) acts as plating mask and prevents the deposition outside the desired structures. However, metal depositions at defects in the dielectric layer (e.g. cracks or pinholes) occur, which is commonly referred to as "background plating", "ghost plating", "parasitic plating" or "overplating". Background plating needs to be strictly avoided, as it reduces the efficiency of the solar cell and moreover results in yield loss due to aesthetic reasons [6–10].

Current methods to evaluate background plating include optical investigation by eye [11]. This method gives a quick qualitative impression of the amount of background plating. However, with this method it is difficult to quantify background plating precisely. Additionally, it is very difficult to detect very small amounts of background plating. Another method is the inspection of the solar cell at random locations with a microscope. This method has also been used to quantify pinholes in the passivation layer [12]. However, a microscopic investigation is typically restricted to very small areas and the extrapolation of the metallized area of the whole wafer is subjected to statistical uncertainties. Additionally, background plating may be very inhomogeneously distributed across the whole wafer, e.g. occurring only at a single scratch on the wafer surface.

Here, the method "MetDetect" is introduced to measure metallized areas of large-area solar cells using a simple and inexpensive setup. The metallized area of a plated solar cell front side includes contact fingers, busbars and the background plating. The method uses a digital image of the front surface of the metallized solar cell obtained by scanning the solar cell with a common flatbed scanner. The image is subsequently edited using an image processing algorithm, yielding the percentage of metallized area to the full-area of the solar cell. To determine the area covered by background plating, "MetDetect" requires a sufficiently high-resolution image of the solar cell which results in a large file size (> 1 gigabyte). Therefore, the processing algorithm is optimized allowing a fast and reliable detection using a conventional office computer.

The method is demonstrated by comparing a detected image to a microscope image obtained at the same location. Furthermore, a correlation between the measured metallized area and short-circuit current density ($J_{SC}$) of the particular solar cells is shown. The used solar cells also show a correlation between measured metallized area and open-circuit voltage ($V_{OC}$) due to pinholes or cracks in the passivation layer. "MetDetect" was also applied to detect the removal of background plating during Sn-plating with an acidic electrolyte (pH of ~1). Here it was observed that the Sn-plating does result in visible plating, however the weight of the solar cell did not increase. A further inspection with "MetDetect" revealed that the metallized area was in fact reduced during the Sn-plating due to a removal of background plating. This removal resulted in an increased $J_{SC}$.

## 2. Workflow of "MetDetect"

In this section the measurement method "MetDetect" is explained in detail. Figure 1 shows a schematic overview of the steps involved in the method.

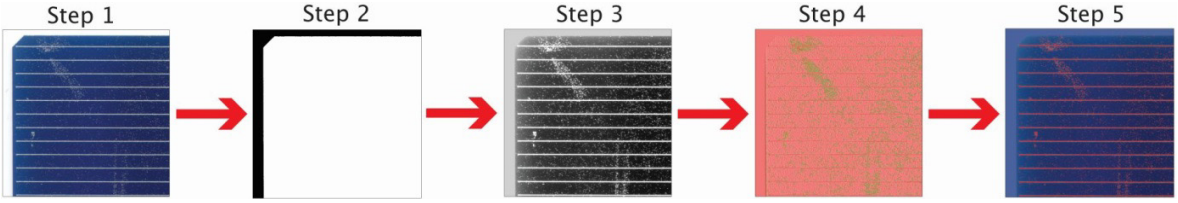


Fig. 1 Overview of the steps applied to determine the total metalized area by "MetDetect". In Step 1 a high resolution image of the wafer is obtained. The white background surrounding the wafer is then removed in Step 2. Step 3 enhances the contrast of the image to separate the metallized and the non-metallized area parts and Step 4 enhances the contrast of local features. Step 5 shows an image of the wafer with the replaced white background and an overlay of the detected plated areas (red).

Step 1: A flatbed scanner takes a color image (red, green and blue channel) of the solar cell by scanning the illuminated solar cell with a line array of photodiodes. The flatbed scanner (Perfection V37, Epson) used in this work, had a resolution of ~30 µm per pixel. The obtained image is then processed with the developed image processing algorithm.

Step 2: The edges of the wafer are detected by applying a threshold to the red channel of the original image. This generates a binary image, with 1 for the bright pixels and 0 for the blue or dark pixels. The algorithm masks the first few pixels from each edge of the image, with the value 1 to avoid the detection of fingers, busbars or other brighter areas on the wafer. The result is a mask of the white background. This mask is used to substitute the original image background by a blue color which avoids a sharp contrast to the solar cell surface at the edge of the wafer.

Step 3: In step three the contrast between metallized areas and the blue/dark wafer is increased. All three color channels of the image are added and rescaled. Since the plated areas are brighter in the image due to increased reflection, the red, green and blue channel show high values. However, in the case of the wafer surface, which is absorption optimized, all color channels show reduced value.

Step 4: In this step a rank filter is applied to enhance the contrast of small features. For each pixel, the mean value of a local neighborhood of the pixel is obtained and subtracted. This increases the contrast of small features such as background plating.

Step 5: A two-step masking of the metallized area is performed using a global threshold on the red channel after step 3 and another global threshold after step 4. Both thresholds need to be adjusted for different solar cell types. Identical thresholds can be used for similarly processed solar cells (e.g. similar texturisation, anti-reflection coating and metallization). The first part of the masking mainly detects large plated areas such as fingers, busbars or larger connected areas of background plating. The second part of the masking mainly detects small features such as small background plating areas. The percentage of metallized area to the solar cell area is calculated by the number of detected pixels divided by the number of pixels of the image which is additionally reduced by the masked pixels from the edge detection.

## 3. Test of method

The experiment to test the method used multicrystalline *p*-type Si solar cell precursor with a full area Al back surface field on the rear surface and with a size of 156 mm × 156 mm. The solar cell precursors were obtained from an industry partner. The antireflection coating was locally removed for metallization of the grid using laser chemical processing (LCP, Select Dop, RENA). LCP uses a laminar flowing liquid jet to confine and focus a laser beam due to total internal reflection. The liquid jet was pressed with ~150 bar through a stainless steel exit nozzle with diameter of 50 µm. The liquid used in this work was phosphoric acid with a concentration of 60 wt%. The used laser parameters are shown in Table 1.

The contact grid opened with the laser featured 94 fingers with a width of ~50 µm and 3 continuous busbars with an opening width of 1.6 mm.

Table 1. Overview of the used LCP parameters.

| Frequency [kHz] | Pulse duration (FWHM) [ns] | Fluence [J/cm²] | Scribing speed [m/s] | Laser pulse density [13] |
|---|---|---|---|---|
| 200 | 60 | 0.4 | 0.5 | Finger: 16<br>Busbars: 39 |

After LCP opening the plating sequence was applied. The plating process consisted of an HF-dip, Ni-plating and Ag-plating. For all plating processes the light induced plating setup was used and the rear of the solar cell did not get in contact with the electrolyte. The HF-dip was performed with 1% HF solution for 30 s to remove the native silicon oxide layer at the laser openings. It was followed by Ni-plating for 1 min at 400 mA in a Watts-type, acidic (pH ~4) Ni-electrolyte. After plating of the Ni seed-layer the Ag conducting layer was plated for 15 min at 100 mA in a commercially available Ag-electrolyte (pH ~12). All plating experiments in this work were performed at a plating temperature as recommended by the vendor of the electrolyte (50°C for Ni and 35°C for Ag). The current-voltage characteristics of the solar cells under illumination were measured after plating and the metallized area was determined with “MetDetect”. For comparison confocal microscope image (LEXT, Olympus) were obtained.

Figure 2 compares a processed scanned image of the metallized solar cell front side with the detected metallized area indicated in red (left) and a microscope image (right) at the same location.

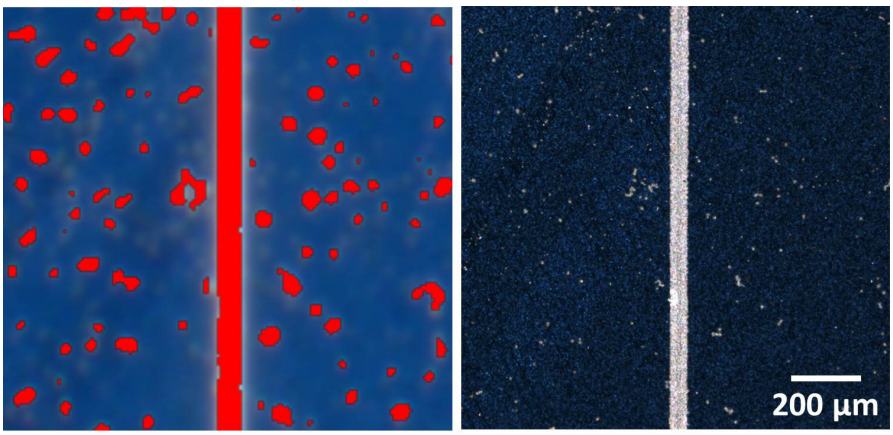


Fig. 2 A scanned image (left) including an overlay of a detected metallized spots by “MetDetect”(red) is compared to a microscope image (right). Both images were obtained at the same location of the wafer. Both images contain a contact finger, which runs vertically through the centre.

The scanned image results in a blurred version of the microscope image due to the lower resolution. The detection algorithm is able to correctly detect most of the larger accumulations of background plating. Only very small or darker background plating was not detected due to the limited resolution of the used scanner. Overall, the measured metallized area overestimated the actual metallized area slightly, which can exemplarily be seen in Fig. 2 were the detected finger is wider than the finger measured with the microscope. The reason for the overestimation of the metallized area is the low resolution of the scanned image and the gleam of the metallized area in the scanned image.

Figure 3 shows the measured $J_{SC}$ of all solar cells in the experiment over the determined metallized area. The solar cells were processed identically. Therefore, the difference in metallized area was predominantly caused by a difference in background plating. The grid accounts for ~6% of the metallized area of all solar cells.

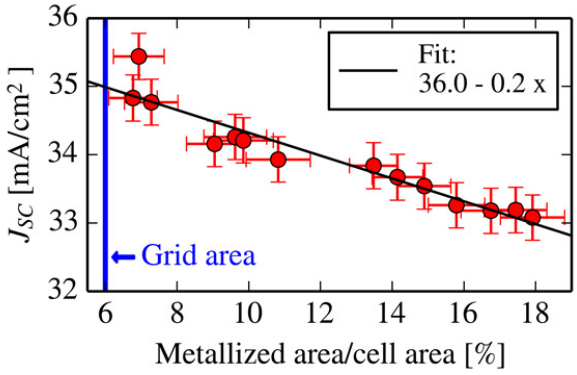


Fig. 3 Short-circuit current density as a function of the determined metallized area. Red denotes the measured $J_{SC}$ with the corresponding error range. The black line represents a fit function of the measured results. The blue line represents the approximate grid area.

The measured $J_{SC}$ increases approximately linearly for decreasing metallized area. This is due to the increased shading caused by the increased metallization and corroborates the applicability of "MetDetect". The linear fit shows that without front surface metallization the theoretically possible $J_{SC}$ of the used precursors is approximately 36 mA/cm².

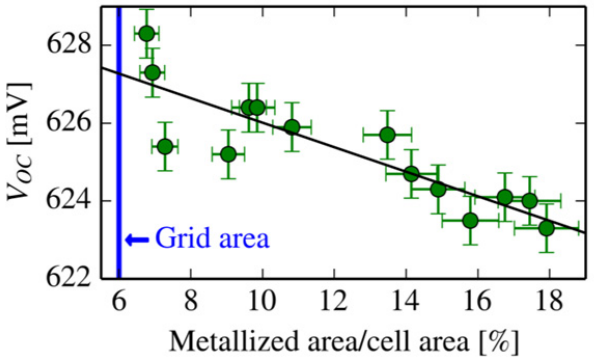


Fig. 4 Open-circuit voltage over the determined metallized area. The green marks are the measured values with the corresponding error range. The blue line represents the approximate grid area. The black line is shown as a guide to the eye.

It was also observed that the metallized area also correlated with the $V_{OC}$ of the solar cells as shown in Fig. 4. The $V_{OC}$ increases for decreasing metallized area. This correlation is most probably not caused by background plating but the amount of background plating is indicative for the amount of pinholes or cracks in the passivation layer. Therefore, "MetDetect" can also be used to quantify pinholes or cracks of the surface dielectric on a large area.

## 4. Removal of background plating

"MetDetect" was applied to corroborate an observation where background plating was removed during subsequent Sn-plating. In this experiment Czochralski-grown silicon solar cell precursors were used, which were obtained from an industry partner. The opening of the solar cells was performed with ps-ablation using an UV-laser with 260 mW and 200 kHz. The laser ablated grid consisted of 3 busbars with a width of 1.5 mm and 120 fingers with a width of 20 µm. Figure 5 shows the processing scheme of these solar cells.

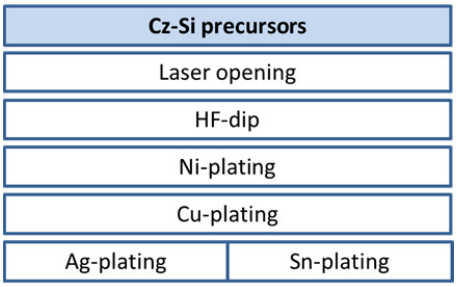


Fig. 5 Processing scheme of the solar cells.

The plating of these solar cells followed the same process as discussed in Sec. 3 for the HF-dip and the Ni-plating. For the conducting layer, Cu was used instead of Ag as shown in Fig. 5. The Cu-plating was performed with a commercially available acidic Cu-electrolyte (pH ~2.8), a plating current of 850 mA (light induced plating setup) for 5 min. The capping layer was plated to guarantee the solder ability of the contacts as the Cu surface would oxidize in contact with air. In this experiment tin and silver were plated as capping layers and compared regarding the effect of background plating. The silver capping layer was plated using the same Ag-electrolyte as discussed in Sec. 3 with a plating duration of 1 min. The tin capping was plated using an acidic Sn-electrolyte based on methane sulfonic acid with a pH value < 1. The solar cell was plated at 200 mA for 1 min (the same duration as for Ag-capping).

Weighing of the solar cells directly before and after the Sn-plating process showed that, despite of the clearly visible Sn deposition on the entire contact grid (color change at the surface), the total weight of the solar cells did not increase. To investigate the underlying reason for the weight discrepancy "MetDetect" was applied to samples before and after the Sn- or Ag-plating processes. For each group 12 solar cells were measured. Table 2 shows the average measured metallized areas and the average results of current-voltage measurements under illumination. The grid accounts for ~6% of the metallized area of these solar cells.

Table 2. Average metallized area ($A_{met}$), short circuit current density ($J_{SC}$), open circuit voltage ($V_{OC}$), fill factor ($FF$) and efficiency ($\eta$) of the solar cell groups. The results of the best solar cells of each group are also shown.

| | $A_{met}$ [%] | $J_{SC}$ [mA/cm²] | $V_{OC}$ [mv] | $FF$ [%] | $\eta$ [%] |
|---|---|---|---|---|---|
| Cu-plating only | 12.4 | 37.0 | 635 | 79.6 | 18.7 |
| *Best solar cell (Cu)* | *12.6* | *37.0* | *635* | *79.9* | *18.8* |
| Ag-capping | 12.1 | 37.1 | 635 | 79.9 | 18.85 |
| *Best solar cell (Ag)* | *11.4* | *37.1* | *635* | *80.7* | *19.0* |
| Sn-capping | 7.7 | 37.3 | 635 | 79.7 | 18.9 |
| *Best solar cell (Sn)* | *7.3* | *37.4* | *635* | *80.7* | *19.2* |

The solar cells plated only with Cu and the solar cells which received an additional Ag-capping layer show total metallized areas (contact grid + background plating) in the range of 12% of the total solar cell area. However, the solar cells which received Sn-plating as capping layer show a significant lower metallization fraction of ~7.7% by simultaneously similar width and heights of the grid. Therefore, it is concluded that the background plating was removed during the Sn-capping layer plating.

A microscopic analysis confirmed that certain background plating areas aside from the contact grid were removed during the Sn-plating process. Figure 6 shows microscope images before and after Sn-plating at the same location.

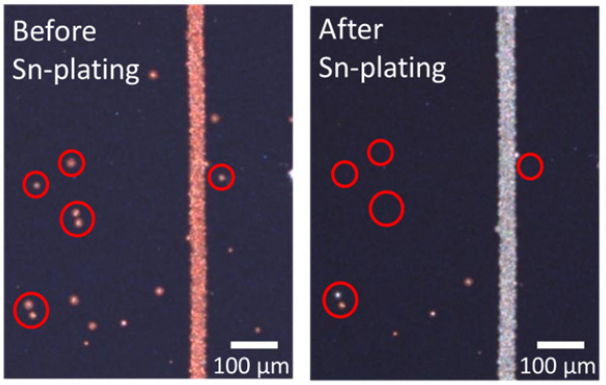


Fig. 6 Top view microscope images of solar cell surface before and after Sn-plating at the same location. Both images contain a contact finger, which runs vertically through the centre. Red circles mark certain background plating particles.

The microscope images show that certain but not the entire background plating was removed during the Sn-plating process. However, the finger and metal grid of the solar cell was plated with Sn. The height and width of the fingers were very slightly increased after Sn-plating as expected (~1 µm).

The reduced metallized area is also observed in the increased $J_{SC}$ in Table 2 for the solar cells with Sn-capping compared to the solar cells with Ag-capping and Cu-plating, only. This resulted in an increase of the average efficiency for the solar cells with Sn-capping. The slightly higher $J_{SC}$ of the solar cells with Ag-capping compared to the solar cells with Cu-plating may be attributed to an enhanced light reflection at the flanks of the finger onto the neighboring silicon surface.

On the contrary to the short circuit current density the $V_{OC}$ of the different groups in Table 2 does not show a difference. This supports the assumption that not the background plating but the defects in the passivation layer, which cause the background plating are responsible for the $V_{OC}$ loss. The *FF* of the solar cells with Cu-plating is the lowest since the Ag and Sn-capping increase the conduction of the grid. Ag is a better conductor than Sn [$\sigma_{Ag}$ = $61.35 \times 10^6$ A/(Vm), $\sigma_{Sn}$ = $8.69 \times 10^6$ A/(Vm)], therefore the benefit in *FF* is largest for this group. Not shown is the *pFF*, which is identical for all groups.

The reason for the removal of background plating is still subject to further investigations. An initial analysis shows that certain background plating particles are removed completely while others are plated with Sn. This suggests that an etching at either the Cu-Ni or the Ni-Si interface may take place. A removal of background plating particles was not observed when the solar cell was only exposed to the Sn-electrolyte without applying plating current. However, it was observed that an etching occurs when a current or voltage is applied as in the case of Sn-plating [14, 15].

## 5. Summary and conclusion

This work introduces a new method ("MetDetect") to quantify the metallized area of standard 156 mm x 156 mm silicon wafer solar cells. "MetDetect" is simple, fast and in-principle inline capable: A solar cell is scanned with a commercially available flatbed scanner and the metallized area is obtained by a developed image processing algorithm. A validation of the obtained results with a microscope analysis and short-circuit current density measurements of solar cells shows that "MetDetect" can accurately detect the metallization fraction and predict short-circuit current density behavior. Additionally it was observed that the open-circuit voltage also correlates with the metallized area due to pinholes and cracks in the passivation layer. The introduced method can be used to quantify metallization from any metallization technique and is especially useful to detect and quantify background

plating. Plating in combination with the inspection method can also be used to quantify pinholes and cracks in the passivation layer.

In the last part of this work, “MetDetect” was applied to investigate an observation regarding the removal of background plating on solar cells during Sn-plating. It was observed that Sn-plating removed isolated background plating particles, which was verified with a substantial decrease in measured metallization area. A reason for the removal of background plating during Sn-plating is still to be identified.

## Acknowledgements

This work was funded by the German Federal Ministry for the Environment, Nature Conservation and Nuclear Safety in the frame of the project rEvolution (FKZ 0325586B).

## References

[1] International Technology Roadmap for Photovoltaic ( ITRPV ) 2013 Results; 2014.
[2] Lennon A, Yao Y, Wenham SR. Evolution of metal plating for silicon solar cell metallisation. Prog Photovolt: Res Appl 2012; 21:1454–1468.
[3] Hörteis M, Bartsch J, Binder S, Filipovic A, Merkel J, Radtke V, Glunz SW. Electrical properties of fine line printed and light-induced plated contacts on silicon solar cells. Prog Photovolt: Res Appl 2010;18:240–248.
[4] Raval MC, Solanki CS. Review of Ni-Cu Based Front Side Metallization for c-Si Solar Cells. J Sol Energy 2013;2013:183812.
[5] Bartsch JM. Advanced Front Side Metallization for Crystalline Silicon Solar Cells with Electrochemical Techniques. PhD thesis, Albert-Ludwigs-Universität Freiburg, Germany; 2011.
[6] Wang S, Lennon A, Tjahjono B, Mai L, Vogl B, Wenham SR. Overcoming over-plating problems for PECVD SiNx passivated laser doped p-type multi-crystalline silicon solar cells. Sol Energy Mater Sol Cells 2012;99:226–234.
[7] Zhou S, Zhou C, Wang W, Zhu J, Tang Y, Chen J, Zhao Y. Comprehensive study of light induced plating of nickel and its effect on large area laser doped crystalline solar cells. Sol Energy Mater Sol Cells 2014;125:33–38.
[8] Zhou S, Zhou C, Wang W, Tang Y, Chen J, Yan B, Zhao Y. Experimental study on the elimination of over-plating problems in industrial manufacturing of large-area acidic-textured laser-doped multi-crystalline solar cells. Sol Energy Mater Sol Cells 2013;108:44–49.
[9] Braun S, Zuschlag A, Raabe B, Hahn G. The Origin of Background Plating. Energy Procedia 2011;8:565–570.
[10] Lee E, Lee H, Choi J, Oh D, Shim J, Cho K, Kim J, Lee S, Hallam B, Wenham SR, Lee H. Improved LDSE processing for the avoidance of overplating yielding 19.2% efficiency on commercial grade crystalline Si solar cell. Sol Energy Mater Sol Cells;95:3592–3595.
[11] Kray D, Bay N, Cimiotti G, Kleinschmidt S, Kösterke N, Lösel A, Sailer M, Träger A, Kühnlein H, Nussbaumer H, Fleischmann C, Granek F, Kosterke N, Losel A, Träger A and Kühnlein H. Industrial LCP Selective Emitter Solar Cells with Plated Contacts. 35th IEEE Photovoltaic Specialists Conference 2010;667–671.
[12] Saint-Cast P, Tanay F, Alemán M, Reichel C, Bartsch J, Hofmann M, Rentsch J and Preu R. Relevant Pinhole Characterisation Methods for Dielectric Layers for Silicon Solar Cells. 24th European Photovoltaic Solar Energy Conference and Exhibition 2009;2084–2087.
[13] Heinrich M, Kluska S, Hameiri Z, Hoex B, Aberle AG. Extracting physical properties of arbitrarily shaped laser-doped micro-scale areas in semiconductors. Appl Phys Lett 2013;103:262103.
[14] Kraft A, Pernia Y, Kalio A, Gautrein A, Ni L, Bartsch J, Glunz SW, Reinecke H. Origin of corrosion effects in solar cell contacts during electrochemical nickel deposition. J Appl Electrochem 2014;45:95–104.
[15] Kraft A, Labusch L, Ensslen T, Dürr I, Bartsch J, Glatthaar M, Glunz SW, Reinecke H. Investigation of Acetic Corrosion Impact on Printed Solar Cell Contacts. Accepted Publication J Photovoltaics 2015.